As originally published in the IPC APEX EXPO Proceedings.

HDPUG Pb-Free Board Materials Reliability Project 2
Moisture Sensitivity and Its Effect on Delamination

C. Xu, R. Kopf, J. Smetana, D. Fleming,
Alcatel-Lucent
Murray Hill, NJ and Plano, TX, USA

Abstract
As part of High Density Packaging Users Group (HDPUG) Pb-Free Board Materials Reliability Project 2, the moisture sensitivity of various lead-free laminates and the effect of moisture uptake on the material survivability through Pb-free reflow were studied using capacitance measurements and time-domain reflectometry (TDR) impedance measurements. WIC-20 coupons were used as test vehicles. In this paper, results from 20 different laminate materials will be summarized. The relationship between moisture uptake and material survivability through Pb-free reflow will be discussed.

1. Introduction

Moisture uptake in laminates is known to affect the thermal stability of printed circuit boards during the soldering process and consequently the long-term reliability of the product. The moisture uptake also changes the dielectric environment of signal traces and affects both impedance and signal loss characteristics of the circuit boards, especially for RF and high speed signals. However, the effects of the absorbed moisture on the dielectric properties of a PWB material is not as dramatic as might be expected [1]. Pre-assembly baking of the bare boards is often used to remove the moisture and therefore minimize delamination during soldering [2]. As there is no simple and quick way to determine the moisture content in a particular circuit board, the selection of baking time and temperature is more of a trial and error process. This is a balance between reducing the moisture content to an acceptable level but not degrading the board materials resulting in other issues (such as solderability issues of board finish).

Both weight gain and capacitance measurements have been successfully used to monitor moisture uptake in the laminate [3, 4]. Capacitance changes due to thermal aging have also been used for detecting delamination [3, 4]. As thermal aging results in a capacitance decrease due to both moisture removal and delamination, a 4% rule has been used, which is based on the experience that the capacitance change due to moisture removal is typically less than 4%.

In APEX 2010, Hunt et al reported results on using TDR route impulse energy (RIE) measurements and capacitance measurements for monitoring moisture uptake and delamination associated with thermal aging [4]. Both the RIE measurement and capacitance methods show promise in evaluating the moisture content of printed circuit boards. Capacitance measurements using capacitors of a solid plate design, have the disadvantage of inhibiting the take up of moisture if the plates are near the surface of the PCB. RIE coupons have an aspect ratio which enables them to be easily incorporated into the break-off panel that commonly occurs around the outside of many PCB designs during manufacture. Provided that similar coupons have been previously characterized in the dry condition, and the PCB has the same build characteristics, both types of coupon can be evaluated immediately prior to assembly to determine the current moisture content level.

In this paper, the moisture sensitivity of twenty Pb-free laminates and the effect of moisture uptake on the material survivability through Pb-free reflow were studied using capacitance measurements and time-domain reflectometry impedance measurements.

2. Experimental

WIC-coupons were used as test vehicles for both capacitance and TDR impedance measurements. Figure 1 shows a top view (left picture in Figure 1) of the WIC-coupon, which includes a 20 by 20 array of through holes on 0.8mm pitch and test points for making TDR impedance and capacitance measurements.

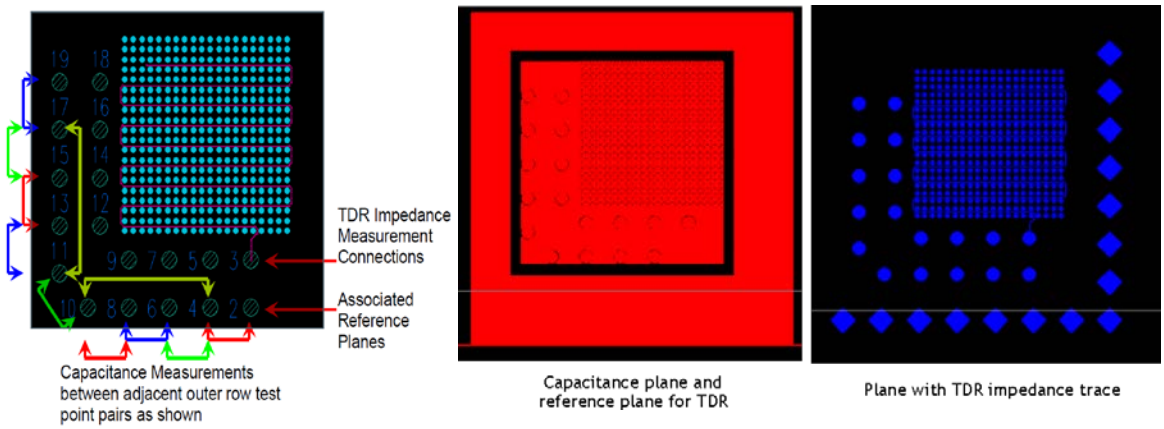

Fig. 1 Top View (left) and Examples of Inner Layer Layout (right) of WIC-20 Coupon

There are two 20 layer constructions, one at 58% resin content, 2.95 mm (.116 inches) thick, that represents a typical 20 layer construction in that thickness, the other is 69% resin content, 3.0 mm (.118 inches) thick, that is representative of a higher layer construction (typically 26-28 layers) in the same thickness. Details of the board construction are available in [7].

Alternate layers include stripline traces surrounded by reference planes for TDR impedance measurements. The reference planes also serve as capacitance planes for the capacitance measurements. TDR Impedance measurements are made on the inner row of test points which are identified by layer numbers 3, 5, 7, 9, 12, 14, 16, and 18 with the associated reference plane for these TDR measurements in the outer row of test points identified by layer numbers 2, 4, 6, 8, 13, 15, 17 and 19. Capacitance measurements are made between the plane pairs identified by the colored pairs of arrows at layers 2 and 4, 4 and 6, 6 and 8, 8 and 10, 10 and 11, 11 and 13, 13 and 15, 15 and 17, 17 and 19. Capacitance measurements are also made between test points for layer 4 and 10, 11 and 17 as shown by the yellow arrow. Figure 1 shows the typical layout of the reference plane (or capacitance plane) in the middle and the plane with impedance trace on the right hand side. It should be pointed out that the Cu reference plane is not continuous and a ring gap is present around every through-hole which serves as the path way for moisture diffusion.

Due to the symmetric construction between the top and bottom side, the capacitance between layers 2 and 4 (A1), 4 and 6 (A2), 6 and 8 (A3), 8 and 10 (A4) are symmetric to the capacitance layers 19 and 17 (A9), 17 and 15 (A8), 15 and 13 (A7), 13 and 11 (A6) regarding their environment and should behave similarly during the aging and reflow test. The capacitance A5 is measured between the two adjacent layers 10 and 11 and is therefore almost twice the value of the other eight capacitance values. In addition to these nine capacitance measurements, the capacitance between layers 4 and 10 (A10), layers 11 and 17 (A11) are also measured. As A10 and A11 represent A2/A3/A4 and A6/A7/A8 in series, respectively, the following equations describe the relationships between these capacitances.

$$1/A10 = 1/A2 + 1/A3 + 1/A4$$

$$1/A11 = 1/A6 + 1/A7 + 1/A8$$

Any changes in A2, A3 and A4 would lead to changes in A10, while changes in A6, A7 and A8 would result in changes in A11.

Capacitance measurements were performed with a Hewlett Packard 4284A Precision LCR meter at 1MHz with a 1V bias. Calibration was performed for the open and short conditions. Both Cp-D and Cs-D measurements were performed. There was no difference between the Cp and Cs measurements, so only the Cp-D results are reported here. A hand-held probe was made to accommodate the 2 different probing distances.

Time Domain Reflectometry (TDR) measurements were performed with an Agilent N1020A TDR probe and Agilent 54754A module, installed in an Agilent 86100C mainframe. The open-ended differential TDR mode was used. Calibration was performed for open, short and 50 ohms. Measurements were preformed at 1GHz and 2GHz. Results from measurements made at 2GHz are very similar to, but much noisier than the results at 1GHz. Therefore, the majority of the measurements were made at 1GHz. The hand-held N1020A TDR probe is designed for on-board measurements and has a variable pitch to accommodate different distances between probing points. The WIC-20 coupon design has a separation of 4mm between the impedance test points. All calibrations were performed with this 4mm distance between the signal and ground pins.

WIC-20 coupons were reflowed using Heller 988C reflow oven. Figure 2 shows the reflow profile used in this work.

3. Results and Discussion

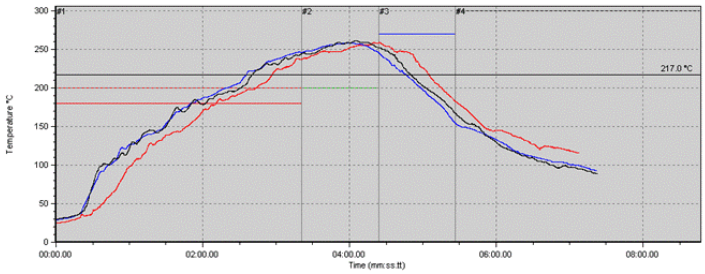

Fig. 2 Reflow Profile

3.1 Phase 1: Feasibility Study

In the first phase of the experiment, four sets of samples were used for determining the optimal measurement parameters as well as the sensitivity of capacitance measurements and TDR impedance measurements for detecting delamination during the Pb-free reflow. Two of the four samples are known to be susceptible to delamination during the reflow.

3.1.1 Capacitance Measurement Feasibility Study

Six coupons of each sample were divided into two groups. Group one (three coupons) was baked at 125°C for 24h and then subjected to 6 cycles of Pb-free reflow. Capacitance measurements were done before and after reflow. Group two (three coupons) was baked at 125°C for 24h, aged at 85°C/85%RH for 7 days and then subjected to 6 cycles of Pb-free reflow. Capacitance measurements were done before 85°C/85%RH aging and after reflow. Group one examines only the thermal effect on delamination of the samples, while group two studies the effect of both moisture uptake and reflow on delamination of the circuit boards. In Figures 3 and 4, capacitance changes are plotted vs. measurement points for all four sets of samples in the two groups.

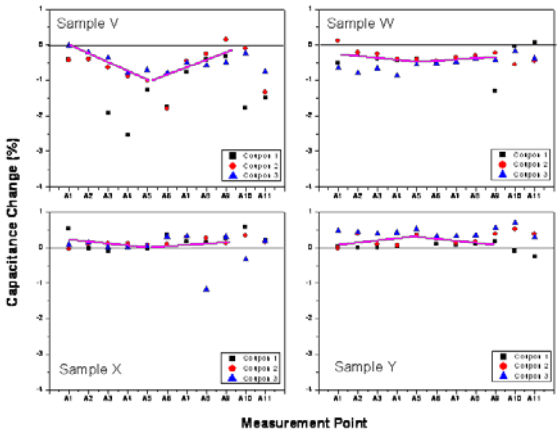

Fig. 3 Capacitance change between immediately after drying and after reflow

As expected from the symmetric construction of the test vehicle (see experimental section), capacitance A1, A2, A3 and A4 behave similar to A9, A8, A7 and A6, respectively. As A10 tracks A2/A3/A4 and A11 tracks A6/A7/A8, A10 and A11 should also behave similarly during the aging.

For the samples without 7 days of 85°C/85%RH aging, most of the measurement points from A1 to A9 lie on a symmetric curve indicated by the magenta lines. The shape of this symmetric curve is determined by the ingress and egress of the moisture into and from the individual laminate layers during aging. To facilitate the discussion, this symmetric curve will be called the capacitance change due to moisture (CCDM) curve in this paper.

Similarly, CCDM curves can be drawn for the four sets of samples from group two (with 7 days 85°C/85%RH aging prior to reflow) in Figure 4. For samples X and Y, all of the measurement points from A1 to A9 also lie on the CCDM curve with minor deviation. For samples V and W, the capacitance changes on the outer layers (A1, A2, A8 and A9) follow the CCDM curve nicely. However, there is a significant deviation from the CCDM curve for the capacitance change of the inner layers (A3, A4, A5, A6 and A7). This large deviation from the CCDM curve is due to delamination of the samples and can be used to detect and quantify (at least semi-quantitatively) the level of delamination. The localization of a large deviation to the inner layers is consistent with the fact that the delamination due to Pb-free reflows generally occurs within the inner layers rather than outer layers of a multilayer circuit board.

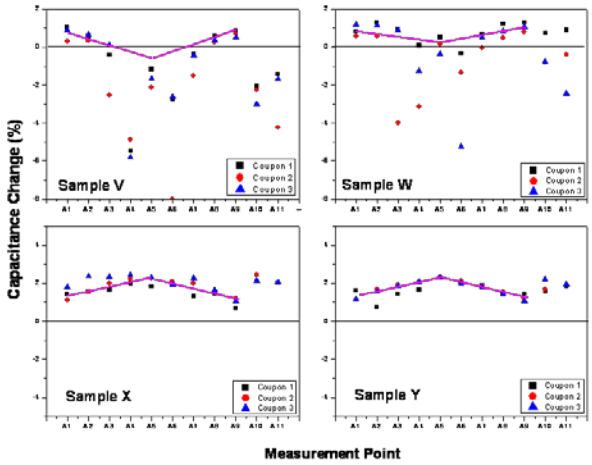

Fig. 4 Capacitance change between immediately after drying and after humidity aging + reflow

Thermal aging such as assembly reflow will remove the moisture and can simultaneously generate delamination in the laminates. Both moisture removal and delamination will decrease the effective dielectric constant of the laminate and lead to an apparent capacitance decrease in both cases. It is important to separate the two effects for accurate delamination analysis using capacitance measurements. Fortunately, moisture ingress/egress occurs uniformly and can be described by the CCDM curve for a given board construction. The delamination, on the other hand, is generally not uniform across the various layers and occurs primarily in the inner layers. The plot of capacitance change versus each layer and the use of CCDM curve provide an effective tool for separating the capacitance change due to delamination from the capacitance change due to moisture removal and will be used throughout this paper.

If we look at the results for samples without 7 days of 85°C/85%RH aging in Figure 3 more carefully, several points deviated from the CCDM curve. For sample V, measurement points A3, A4, A6 for coupon one and A6 for coupon two show a 1-2% deviations from the CCDM curve and could be due to delamination. Further confirmation comes from measurement points A10 and A11. Consistent with the deviation of measurements points A3, A4 and A6 for coupon one, both A10 and A 11 also show a 1-2% deviation. For coupon 2, on the other hand, only A11 shows a significant deviation, tracking the A6 result on the same coupon.

In Figure 3, there are also several other points deviating from the CCDM curve. For instance, A9 on coupon one for sample W and A8 on coupon three for sample X show significant deviation from the CCDM curve. However, these deviations are not seen in the corresponding A11 measurement. This suggests that the deviation in these two particular cases is most likely due to measurement error, as only a single capacitance measurement was done for each point.

In order to confirm that the 1% deviation of the measured capacitance change is indeed due to delamination, cross sections were done on a reference sample (as received sample without any aging), and coupons one and two for sample V. Figure 5 indicates the locations of the five cross sections performed on each coupon. Consistent with the capacitance measurement results, many cracks and delamination were observed on layers A3, A4 and A6 for coupon 1 and on layer A6 for coupon 2. No sign of delamination was seen on the reference sample.

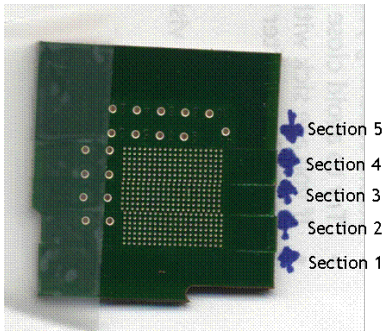

Fig. 5 Locations of the cross section

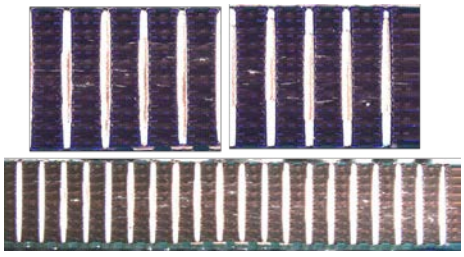

Fig. 6 Cross section of coupon one

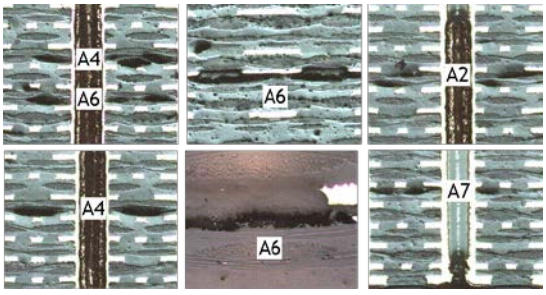

Fig. 7 Cross section of coupon one

In Figures 6 and 7, selected results for coupon one are shown, while Figures 8 and 9 summarize the results for coupon two. Interestingly, a few small cracks were also observed in several other layers, where no significant capacitance change was measured.

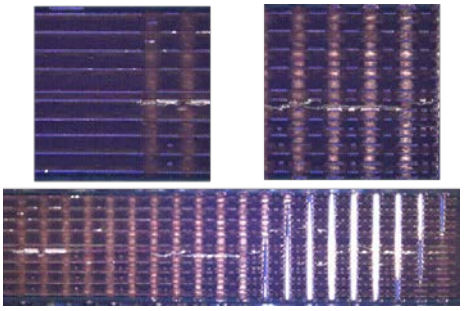

Fig. 8 Cross section of coupon two

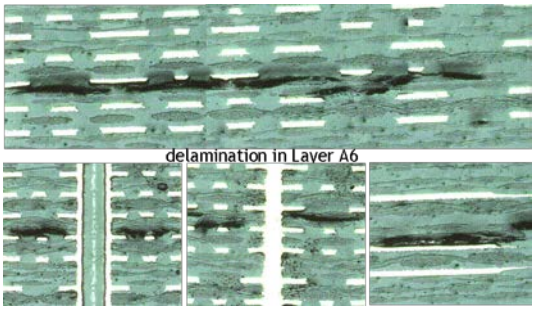

Fig. 9 Cross section of coupon two

In order to compare the cross section results with the measured capacitance change in a semi-quantitative manner, the length of all the delamination segments seen on the five cross sections for each coupon were measured. Then the sum of all the lengths for each capacitance layer is used as a semi-quantitative measure for the degree of delamination in that particular layer. This is clearly a crude estimation of the degree of delamination in each layer, as it uses a one dimensional parameter (length) to represent a three dimensional parameter (void volume due to delamination) and the measurement was only done on five cross sections. Nevertheless, it provides a useful, semi-quantitative comparison. Figure 10 compares the degree of delamination as measured by the length of cracks observed in the cross section with the degree of delamination as measured by the capacitance change for each layer in coupons one and two. As one can see in Figure 10, there is a rather good correlation between the cross section and capacitance measurements.

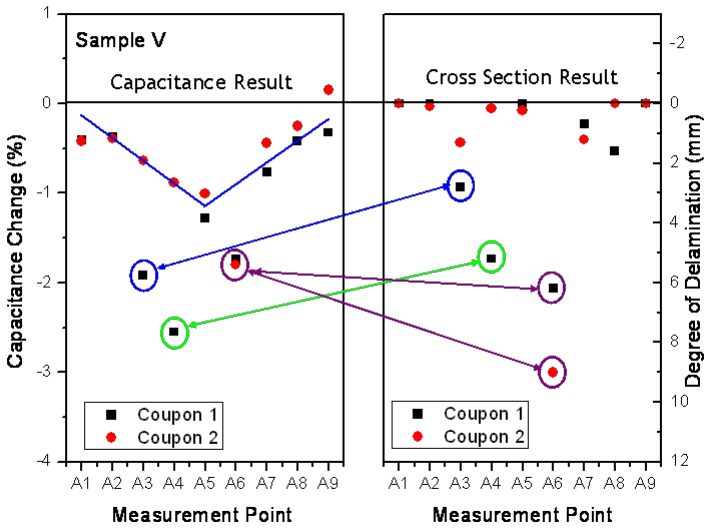

Fig. 10 Correlation of delamination observed in the cross section with that in the capacitance measurement

The four delamination layers predicted by capacitance measurement results (A3, A4 and A6 for coupon 1 and A6 for coupon 2) show the highest degree of delamination in the cross section. However, the capacitance measurements failed to detect the low level delamination seen in the cross section, such as delamination in A7, A8 for coupon one and A3, A7 for coupon two.

It is useful to estimate the detection limit using capacitance measurements for detecting delamination. The delamination detection using capacitance change is based on the fact that delamination produces voids. These voids decrease the apparent dielectric constant of the laminate and increase the distance between the two copper plates used for the capacitance measurement. Both lead to a capacitance decrease. The relative capacitance change can be estimated using following equation:

$$(C_d\text{-}C)/C=(\varepsilon_d/D_d-\varepsilon/D)/(\varepsilon/D)=(\varepsilon_d D-\varepsilon D_d)/(\varepsilon D_d)=(D\Delta\varepsilon-\varepsilon\Delta D)/\varepsilon(D+\Delta D) \quad (1)$$

Where:
C: Capacitance before delamination
C_d : Capacitance of delaminated layers.
D: Distance between the two copper planes
D_d : Distance between the two copper planes of delaminated layers.
$\Delta D=D_d-D$: distance change due to delamination
ε : Dielectric constant of the laminate
ε_d: Dielectric constant of the laminate with delamination
$\Delta\varepsilon=\varepsilon_d-\varepsilon$: Dielectric constant change due to delamination

For small changes of the distance between the two Cu planes, the following approximation can be used:

$$(C_d\text{-}C)/C=\Delta\varepsilon/\varepsilon-\Delta D/D \quad (2)$$

The average relative distance change can be related to percentage of void in the laminate using the following equation:

$$\Delta D/D=-V_{air} \quad (3)$$

V_{air}: volumetric percentage of void in the laminate due to delamination:

The dielectric constant change due to void formation can be described by Lichtenecker's mixing rule [5]:

$$\varepsilon_d^{\alpha}=V_{air}+(1-V_{air})\varepsilon^{\alpha} \quad (4)$$

α : a parameter that determines the type of mixing rule.

when $\alpha = 1$, a parallel mixing rule is operating:

$$\varepsilon_d = V_{air} + (1 - V_{air})\,\varepsilon \quad (5)$$

When $\alpha = -1$, one has a serial mixing rule:

$$1/\varepsilon_d = V_{air} + (1 - V_{air})/\varepsilon \quad (6)$$

Serial and parallel mixing rules give lower and upper limits of the dielectric constant between the capacitance layers with void. Capacitance change due to delamination can then be estimated for the two extreme cases as following:

For parallel mixing rule, equation (2) can be combined with equations (3) and (5):

$$(C_d - C)/C = V_{air}\,(1 - \varepsilon)/\varepsilon + V_{air} \quad (7)$$

For a typical dielectric constant of 3.5 to 4, relative capacitance change can be estimated using:

$$(C_d - C)/C = -(1.71 \text{ to } 1.75)\,V_{air} \quad (8)$$

For serial mixing rule, equation (2) can be combined with equations (3) and (6):

$$(C_d - C)/C = (V_{air} - \varepsilon\,V_{air})/(\varepsilon\,V_{air} + 1 - V_{air}) + V_{air} \quad (9)$$

For a typical dielectric constant of 3.5 to 4, relative capacitance change can be estimated using:

$$(C_d - C)/C = -(4 \text{ to } 5)\,V_{air} \quad (10)$$

Equations (8) and (10) indicate that a 1% void formation due to delamination will lead to a relative capacitance change somewhere between 1.7% and 5%, depending on the dielectric constant and the mixing rule at work. As 1% of capacitance change is the detection limit for delamination under the experimental conditions used in this work, 0.2% to 0.6% of void formation due to delamination is required so that it can be detected by the capacitance change. As the delamination typically extends in the x and y directions rather than z-direction, the dielectric change due to delamination follows serial mixing rule more than parallel rule. Therefore, the detection limit is closer to 0.2% than 0.6% under the experimental conditions used in this work. It is important to keep this detection limit in mind as one uses capacitance to evaluate the robustness of various materials during the Pb-free reflow. Clearly, this detection limit can be improved by optimizing test vehicles and improving precision of the capacitance measurement.

3.1.2 TDR Impedance Feasibility Study

Similar to the capacitance, TDR impedance is also sensitive to the dielectric environment of the stripline and has been proposed by IBM for detecting delamination [6]. An advantage of TDR impedance measurements over capacitance measurements is its ability to provide the exact location of the delamination. The capacitance measurement is averaged over the entire area between the two copper planes and can only detect the layer location of the delamination without information on its x or y location. For the TDR impedance measurement, the time domain reflectance spectrum is measured over the stripline. If delamination is present near a certain point on the stripline and causes the impedance change, it will be reflected at that point in the spectrum, hence the location sensitivity of the method.

TDR impedance measurements were conducted at 1 GHz and 2 GHz. Similar results were obtained for both frequencies with the results at 2GHz showing a higher level of noise. Therefore, only results taken at 1GHz will be presented in this paper. As only samples V and W showed significant delamination after 6 cycles of Pb-free reflow, we will focus on these results first. Figure 11 shows TDR impedance measurement results for sample V after drying at 125°C (left image) and 6 cycles Pb-free reflow following 7 days aging at 85°C/85%RH (right image). There are 24 curves for each sample (8 measurement points for each of the three coupons). For reference, TDR impedance results for the calibration standards 25, 50 and 75 ohms were also included. The impedance mismatch observed at time zero is due to the connection between the TDR probe and the WIC-20 coupons, while the reflection near 2ns is due to the termination of the stripline in the WIC-20 coupons. The curve between 0 and 2ns reflects the impedance along the stripline within WIC-20 coupons. As one can see in Figure 11, no change was observed for the 24 impedance curves between the samples after reflow and before reflow, even though significant delamination was present on these samples.

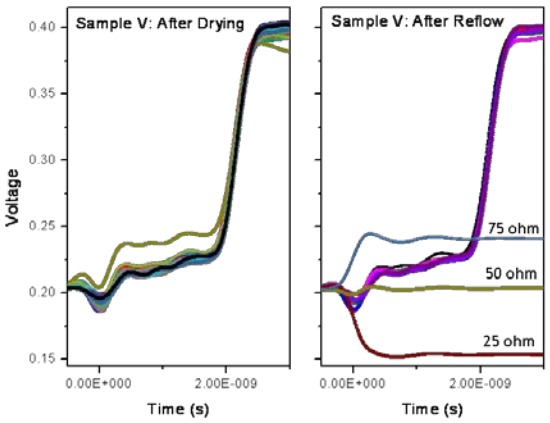

Fig. 11 TDR impedance result for sample V after drying (left) and after humidity aging and reflow (right)

In order to create even more delamination in the samples for TDR measurement, 4 days of additional humidity aging, followed by 3 cycles of assembly reflow were applied on samples V and W. Figure 12 compares capacitance changes for samples after 9 reflows with samples after 6 reflows. Clearly, significantly more delamination was generated in the samples after 9 cycles of reflow compared to the samples after 6 reflows.

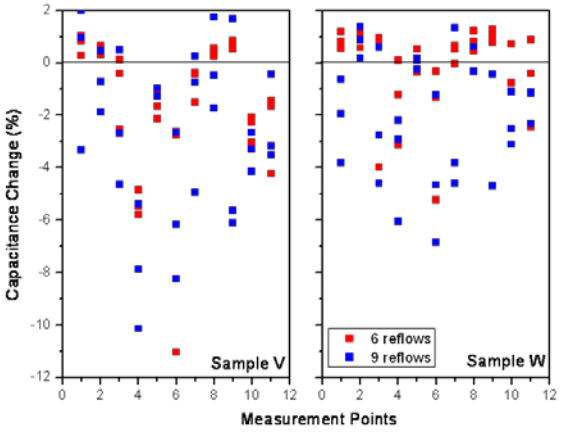

Fig. 12 Comparison of capacitance changes after 6 (red) and 9 reflows (blue) for samples V and W

Figures 13 and 14 show TDR results for samples V and W after both 6 and 9 reflows. Compared to the results before reflow, no significant change which can be related to delamination is seen. This is in contrast to successful detection of delamination using capacitance changes, which are also based on the change of the dielectric environment. There are two possible explanations for this difference. First, the capacitance change was measured between two ground planes averaged over a large area, while the impedance measurement is on an individual point on the stripline for providing lateral resolution. Therefore, the capacitance measurement is several orders of magnitude more sensitive than the impedance measurement. Second, delamination may not have occurred at the interface of the stripline and the adjacent laminate and therefore did not change the impedance significantly.

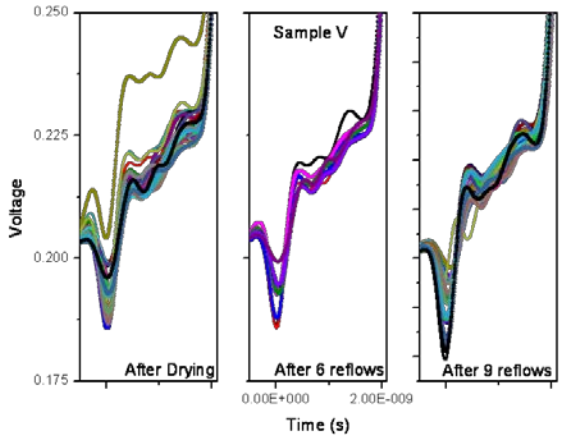

Fig. 13 TDR impedance result for sample V

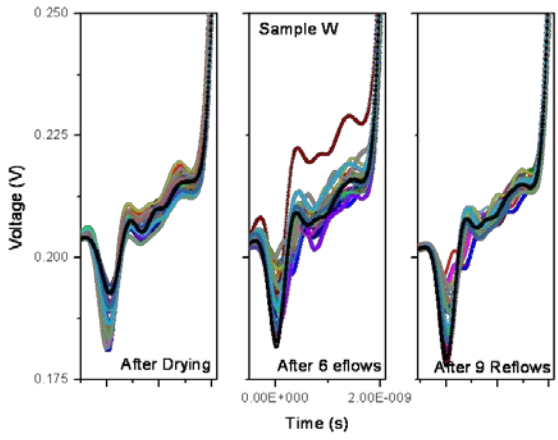

Fig. 14 TDR impedance result for sample W

3.2 Capacitance Measurements on All Samples:

Due to the lack of the success with the impedance measurement, only capacitance measurements were performed in the phase II experiment, where all 27 samples were studied. Table 1 summarizes results for all 27 samples, among which 10 samples are FR-4, 8 samples are halogen free FR-4 and 9 samples are high speed materials. As it can readily be seen in Table 1, none of the FR-4 materials shows delamination indicated in the capacitance measurements. However, about half of the halogen free FR-4 and high speed materials showed varying degrees of delamination under various conditions. In the next few paragraphs, we will divide the samples into several groups and show typical results for each group.

3.2 Samples with delamination

Table 1 Delamination results of all samples under various conditions detected by capacitance or cross section

		After 6X @ 260C Reflow						9X @ 260C
APEX Coding	Resin Content (%)	after drying	cross section	with 168hrs 85C/85%RH aging	Cross section	with 504hrs 85C/85%RH aging	Cross section	
	FR4							
A	58	No		No		No		
B	69	No		No		No		
C	58	No		No				
D	58	No		No		No	No	
E	58	No		No		No		
F	58	No		No				
G	69	No		No				
H	58	No		No		No		
I	58	No		No		No	No	
J	58	No		No				
	Halogen Free FR4:							
K	58	No		No		No	No	
L	69	No		No		No		
M	58	No		Yes				
N	69	No		Yes	yes	Yes		
O	58	No		Yes				
P	58	No		No	No	No		
Q	58	No		No		Yes	Yes	
R	58	No		No	No	No		
	High Speed Materials:							
S	58	No		No	no			
T	69	No		No	no			
U	58	Yes		Yes				
V	58	Yes	yes	Yes				Yes
W	69	No		Yes				Yes
X	58	No		No				
Y	58	No		No				Yes
Z	69	No		No				No
AA	58	No		No				

Only two samples (U and V) showed delamination after 6 reflows on the dried samples. Figure 15 compares capacitance measurement results for samples U and V. For sample U, only one of the three coupons showed significant delamination in the capacitance measurements. Sample V showed delamination on two of the three coupons, although the degree of delamination on sample V is significantly less than sample U based on capacitance measurement results.

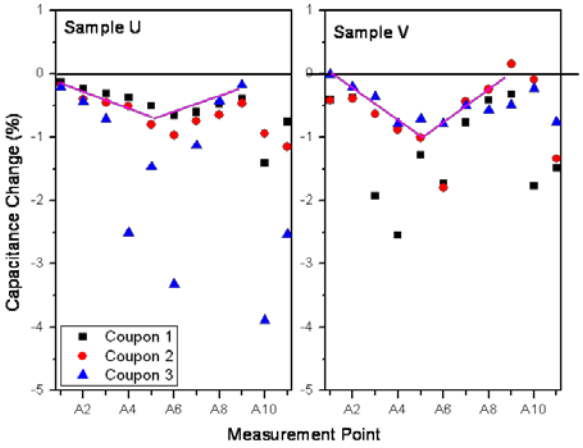

Fig. 15 Capacitance results for samples showing delamination after reflow of the dried coupons

For samples aged for one week at 85°C/85%RH prior to reflow, four additional samples (M, N, O and W) show delamination in addition to samples U and V. The remaining 21 samples did not show delamination based on capacitance changes.

Six of the delaminated samples showed different moisture uptake behavior and can be divided in to three groups. Figure 16 shows representative results for the three groups. For each sample, two sets of capacitance changes were plotted. The top three curves (black, red and blue) are capacitance changes between immediately after drying at 125°C and after 7 days 85°C/85%RH aging. These capacitance changes are solely due to the moisture uptake in the laminate during humidity aging. The three curves on the bottom represent capacitance changes of the same sample between immediately after drying at 125°C and after 7 days 85°C/85%RH plus 6 cycles of reflow.

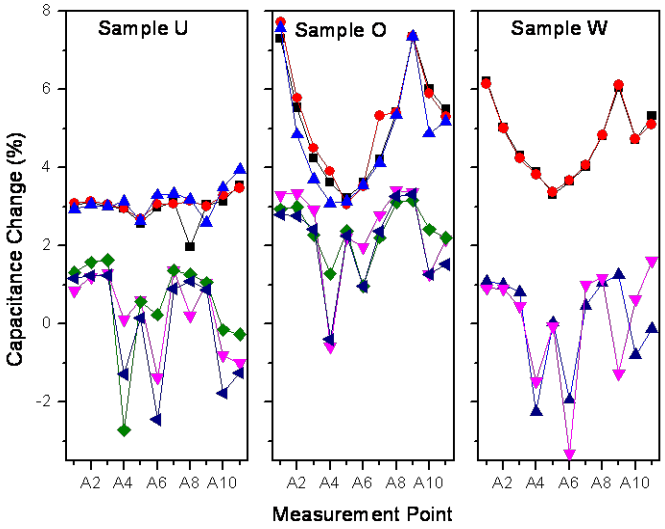

Fig. 16 Capacitance change for samples showing delamination after 7d humidity aging + reflows

Group one contains sample U, which shows almost identical capacitance changes for all of the layers (see graph on the left for sample U), indicating a similar moisture uptake for all of the layers. Group two contains samples M, N and O, which show very different capacitance changes for the individual layers. The result for sample O is provided in the middle graph of Figure 16. While the capacitance change for the two outer layers (A1 and A9) is as high as 7.5%, the capacitance change for

the inner layers (A4, A5 and A6) is only ~3.5%. Group three contains sample V and W and lies somewhere between the first two groups. The result for sample W is provided as the right graph in Figure 16.

As the Cu layer is practically impermeable to moisture, the moisture uptake occurs by water diffusion through the laminates. This can occur either from the edge of the WIC-20 coupon or through the gap between the Cu plated through-holes and the surrounding Cu planes. Due to the much longer diffusion path from the edge compared to the pathway from the top/bottom surface of the coupon, the moisture uptake occurs primarily through the gaps surrounding the through-holes. In case of laminate O, the water absorption is rapid but the water diffusion through the laminate is relative slow, resulting in a much higher moisture uptake in the outer layers compared to the inner layers. For sample U, the water diffusion through the laminate is similar to or faster than the water absorption and leads to a similar moisture uptake across inner and outer layers of the coupon. This difference is most likely due to the stronger interaction of water molecules with laminate O than with laminate U.

In contrast to their rather different moisture uptake behavior, all three samples showed similar delamination propensity. Furthermore, the location of the delamination is also similar for all three samples and is in layers A4 and A6. This is clearly related to the construction of the WIC-20 coupons. A4/A6 layers are the location of the highest thermal mechanical stress during reflow. The absolute water content plays only a secondary role.

In order to confirm the capacitance measurement results, cross section were also performed on five (N, P, R, S and T) of the twenty seven samples. This result is also summarized in Table 1. Consistent with the capacitance measurements, only sample N showed significant delamination. However, eyebrow types of defects were also seen for samples S and T that were not detected by the capacitance measurements.

3.3 Samples without delamination

The capacitance change results (see summary in Table 1) indicate that twenty one of the twenty seven samples showed no significant delamination (less than 0.2-0.6% voids formation) after 7 days 85°C/85%RH aging and 6 cycles of Pb-free reflow. Similar to the delaminated samples, the twenty one samples without delamination can also be divided into three groups based on the moisture uptake behavior. In parallel to Figure 16, Figure 17 shows representative results for each group. Two sets of capacitance change results were also included for each sample in Figure 17:

Set 1: capacitance change between the sample after drying at 125°C and after 7 days 85°C/85%RH (top curves)
Set 2: capacitance change between the sample after drying at 125°C and after 7 days 85°C/85%RH plus 6 cycles of reflow (bottom curves).

Samples Y, Z and AA in group one show similar moisture uptake across both inner and outer layers, as the left graph in Figure 18 illustrates. Samples A, B, E, F, G, H, I, K, L, P, Q and R in group two show high moisture uptake in the outer layers and low moisture uptake in the inner layers (see the graph in the middle of Figure 17). Samples C, D, S, T, J and X in group three lie somewhere between the first two groups (see the graph on the right in Figure 17). Again, the different moisture uptake behavior is most likely due to the difference in the interaction between the laminates and water molecules. The different moisture uptake behavior of these three groups of laminates without delamination mirrors that of the three groups of the laminates with delamination described in section 3.2. This result indicates that there is NO correlation between the moisture uptake behavior of a laminate and its delamination propensity.

As the group two samples show significantly less moisture uptake in the inner layers compared to the outer layers (see the middle graph in figure 17), one may ask the question: Would the delamination occur after reflow if there is high moisture uptake in the inner layers on these samples? In order to address this question, a subset of these laminates was subjected to 3 weeks humidity aging at 85°C/85%RH prior to the Pb-free reflow. Among the 12 samples (A, B, D, E, H, I, K, L, N, P, Q and R) selected for extended humidity aging, 10 samples (A, B, E, H, I, K, L, P, Q and R) are from group two, which showed no delamination after one week humidity aging and reflows. Sample N is also from group two but showed delamination after one week humidity aging and reflows. Sample D was from group three.

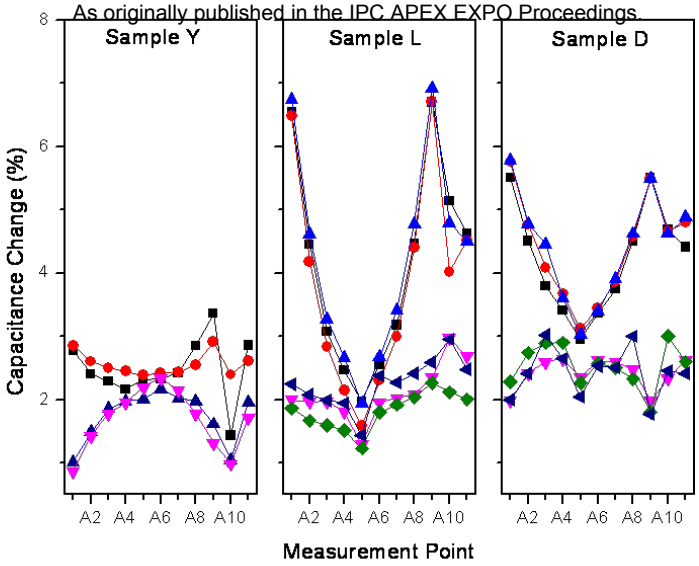

Fig. 17 Capacitance change for samples showing no delamination after 7d humidity aging + reflows

After three weeks humidity aging at 85°C/85%RH and 6 cycles of Pb-free reflow, only one sample (Q) out of the 10 samples from group two showed minor delamination. Sample N also showed delamination after the extended humidity aging, consistent with the result after one week humidity aging. Sample D from group three did not show delamination after the extended aging either. This result is also summarized in Table 1.

Figure 18 shows selective results for three of the ten samples from group two. For each sample, two coupons were used. Capacitance measurements were performed immediately after drying at 125°C, after one week humidity aging, after three weeks humidity aging, and finally after 6 cycles of reflow. Three sets of capacitance changes are plotted in Figure 18:

Set 1: capacitance change between the sample after drying at 125°C and after 7 days 85°C/85%RH (black and red curves)
Set 2: capacitance change between the sample after drying at 125°C and after 21 days 85°C/85%RH (blue and magenta curves)
Set 3: capacitance change between the sample after drying at 125°C and after 21 days 85°C/85%RH plus 6 cycles of reflow (navy and olive curves).

As it can clearly be seen in Figure 18, the inner layers of all the coupons showed significantly higher moisture uptake after three weeks of humidity aging than after one week of humidity aging. However, only one coupon out of the 20 coupons from the ten group two samples showed delamination as indicated by the deviation of the capacitance change in the navy curve for sample Q. The deviation of A3 for sample Q is also confirmed by the deviation of A10 on the same coupon. This result indicates again that moisture uptake behavior has only a secondary effect on the delamination propensity of group two laminates.

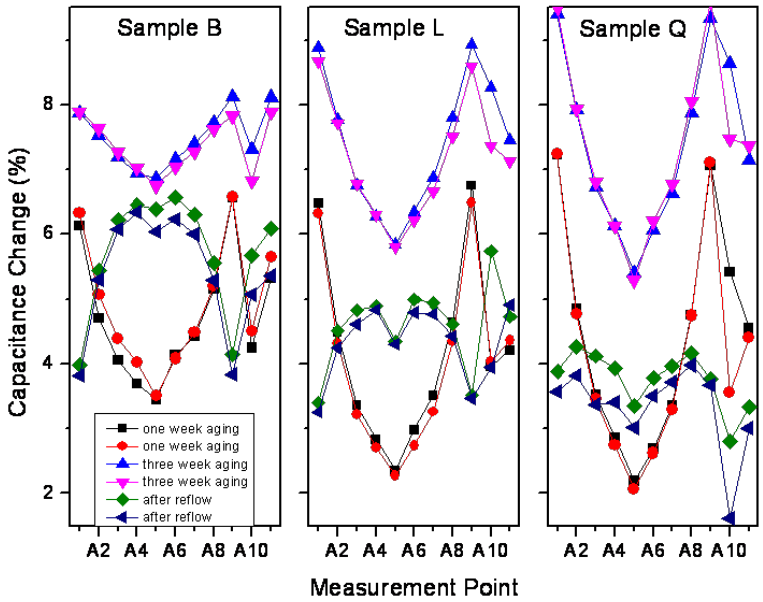

Fig. 18 Capacitance change for samples subjected to extended humidity aging

In order to confirm the capacitance measurement results, cross sections were also performed on four (D, I, K and Q) of the ten samples subjected to extended humidity aging. This result is also summarized in Table 1. Consistent with the capacitance measurement, only sample Q showed significant delamination. However, eye brow and cigar void were also seen for samples D and I but were not detected by the capacitance measurement.

3.3 Samples with different resin content

As mentioned above, there are two 20 layer constructions, one at 58% resin content with alternating 1080 and 2116 glass fibers, the other is 69% resin content with alternating 1080 and 106 glass fibers. Both constructions have similar thicknesses: 2.95 mm thick vs. 3.0 mm thick. Details of the board construction are available in [7]. Seven laminates were built with both constructions. Samples A and B, F and G, K and L, M and N, S and T, V and W, and Y and Z have 58% and 69% resins respectively (Table 1). Among the seven pairs of laminates, two pairs (M and N, V and W) showed delamination after 7 days humidity aging plus reflows, while the remaining 5 pairs showed no delamination. Figure 19 shows representative results for three of the seven laminates. Two sets of capacitance change results were included for each sample:
Set 1: capacitance change between the sample after drying at 125°C and after 7 days 85°C/85%RH (top curves)
Set 2: capacitance change between the sample after drying at 125°C and after 7 days 85°C/85%RH plus 6 cycles of reflow (bottom curves).

As expected, samples with 69% resin content (red curves) show consistently higher moisture uptake than samples with 58% resin content (black curves). Despite of the higher moisture content in sample W compared to sample V, sample W showed less delamination than sample V. Similar results have also been observed for samples M (58% resin) and N (69% resin), where sample N showed higher moisture uptake but less delamination than sample M. Interestingly, sample V also showed delamination after reflow of the dried coupons while no such delamination was observed on sample W (see Table 1 and discussion in 3.2). In regard to delamination, samples with 59% resin content seem to be less thermally stabile than samples with 68% resin content. A possible explanation for this difference is the larger resin-glass interface in samples with 59% resin compared to the samples with 68% resin content. Such an interface is often one of the weak links in the multilayer board.

4. Conclusion

Area averaged capacitance measurements can be used to detect delamination created in WIC-20 coupons under the aging conditions used in this work, while localized TDR impedance measurements do not provide sufficient sensitivity. Both moisture removal and delamination during thermal aging decrease the effective dielectric constant of the laminate and lead to an apparent capacitance decrease. Moisture ingress/egress occurs uniformly and can be described by the CCDM (capacitance change due to moisture) curve for a given board construction. Delamination, on the other hand, is generally not uniform across the various layers and typically occurs only in the inner layers.

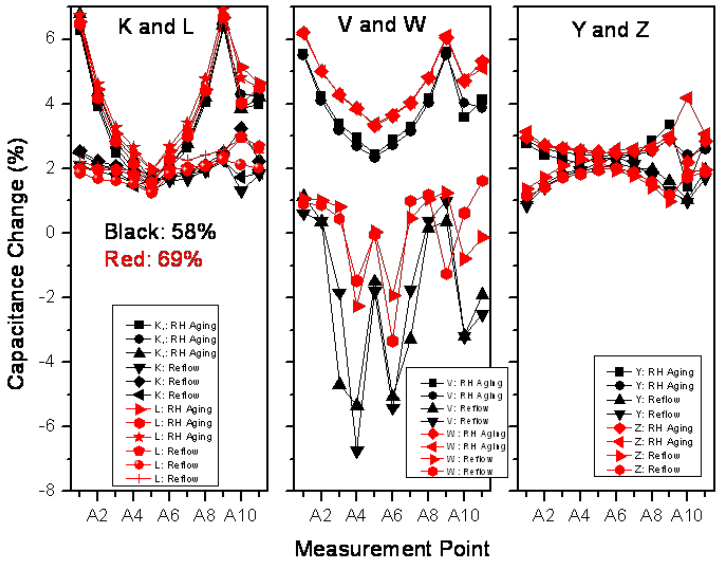

Fig. 19 Effect of Resin Content on Moisture Uptake and Delamination

The plot of capacitance change versus the layers and the use of CCDM curves provide an effective tool for separating the capacitance change due to delamination from the capacitance change due to moisture removal and can be effectively used for delamination detection and semi-quantification of the degree of delamination during assembly reflow.

Using the Lichtenecker Mixing rule, the detection limit of delamination using capacitance change has been estimated to be 0.2-0.6% void formation in the laminate under the experimental conditions used in this work. Delamination, eye brow or cigar voids, which generate less than 0.2% void between the Cu layers, can not be detected using capacitance change measurements. This detection limit can be improved by optimizing the test vehicles and improving the precision of the capacitance measurement, which will be one focus of future work.

The 27 samples showed significantly different moisture sensitivity and moisture uptake kinetics, which are determined by the interaction between laminate and water molecules. Contrary to conventional belief, no correlation between moisture uptake behavior and delamination propensity of the laminates is observed. The primary factor determining the thermal stability of multilayer boards during reflow is the type of laminate. The process condition of the multilayer board, which is not studied in this work, should also have a strong effect on the thermal stability of the board. WIC-20 coupons can be effectively used for monitoring the quality of the multilayer board production and will be further investigated in follow up work. The construction of the multilayer board determines the location of the highest thermal mechanical stress during reflow and therefore the location as well as degree of delamination. For a marginal multilayer board, moisture uptake provides additional stress during the reflow and exacerbates delamination.

5. Acknowledgements

We would like the thank S. Kahn, M. Benowitz, N. Weimann and Y.K. Chen for their continuing support, S. Kahn for proofreading and editing the manuscript. We would also like to thank N. Hoffman and D. Rutkowski from Agilent Technologies for their help with the TDR measurements.

References:

1. J.-M. Heinola and J.-P. Ström, “Evaluation of Dielectric Properties of Printed Wiring Board Materials by Using a Microstrip-ring and Strip-line Ring Resonator Methods”, IEEE Electrical Insulation Magazine, May/June 2007 — Vol. 23, No. 3.
2. Joseph E. Kane, “Weigh/Bake/Weigh Testing To Determine Moisture Content in Printed Boards”, IPC Electronics Midwest 2010.
3. Kerin O’Toole, Bob Esser, Seth Binfield, and Craig Hillman and Joe Beers, “Pb-Free Reflow, PCB Degradation, and the Influence of Moisture Absorption”, APEX 2009.

4. Chris Hunt, Martin Wickham, Owen Thomas and Ling Zou, “Assessment of Moisture Content Measurement Methods for Printed Circuit Boards”, APEX 2010.
5. K. Lichtenecker, Phys. Z., 27, 115 (1926).
6. W. Rothschild, private communication.
7. Smetana, J., Birch, B., Rothschild, W., “A Standard Multilayer Printed Wiring Board for Material Reliability Evaluations”, IPC/APEX, Las Vegas NV, 2011.